5.4 IMPROVED RANGE-VELOCITY AMBIGUITY MITIGATION FOR THE TERMINAL DOPPLER WEATHER RADAR*

John Y. N. Cho*, Nathan G. Parker, and Gabriel R. Elkin
MIT Lincoln Laboratory, Lexington, Massachusetts

1. INTRODUCTION

The Terminal Doppler Weather Radar (TDWR) radar data acquisition (RDA) subsystem is being replaced as part of a broader FAA program to improve the supportability of the system. An engineering prototype RDA has been developed with a scalable, open-systems hardware platform. With the dramatically increased computing power and more flexible transmitter control, modern signal processing algorithms can be implemented to improve the quality of the base data. Nation-wide, the most serious data quality challenge is range-velocity (RV) ambiguity. In a previous study (Cho et al., 2003) we showed that multiple pulse repetition interval (PRI) and constant-PRI phase-code processing have complementary strengths with respect to range-fold protection, and proposed an adaptive waveform and processing selection scheme on a radial-by-radial basis. Here we describe the scheme and give more details about the clutter filtering and velocity dealiasing algorithms to be used on the two types of signals.

2. RDA PROTOTYPE

Fig. 1 shows a simplified block diagram of the TDWR as currently installed at 45 U.S. sites. The digital signal processor (DSP) performs clutter filtering and generates moment data, as well as functioning as a conduit for system control between the Remote Monitoring System (RMS) and the antenna, transmitter, and receiver/exciter (REX) subsystems. The legacy DSP hardware consists of three commercial off-the-shelf (COTS) and 19 custom cards, installed in a single 19" multibus chassis. This technology will soon be unsupportable.

* This work was sponsored by the Federal Aviation Administration under Air Force Contract No. F19628-00-C-0002. Opinions, interpretations, conclusions, and recommendations are those of the authors and are not necessarily endorsed by the United States Government.

Corresponding author address: John Y. N. Cho, MIT Lincoln Laboratory, 244 Wood St., Lexington, MA 02420-9185; e-mail: jync@mit.edu.

A block diagram for the re-hosted RDA hardware is shown in Fig. 2 (Cho et al., 2003). Dual Intel Xeon (currently 3.0 GHz) processor compute servers running Linux perform both the signal processing and system control functions. The system control computer houses a SIGMET RVP8 system that provides a COTS solution for the digital receiver, digital waveform shaping, and timing functions in three PCI cards each with several field programmable gate array (FPGA) chips. A combination of interrupt-driven software and FPGA code allows the system to change PRI and phase coding on a radial-by-radial basis.

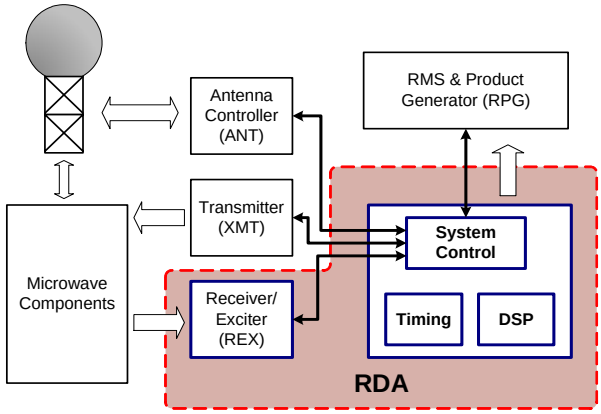

Figure 1. Block diagram of the legacy TDWR.

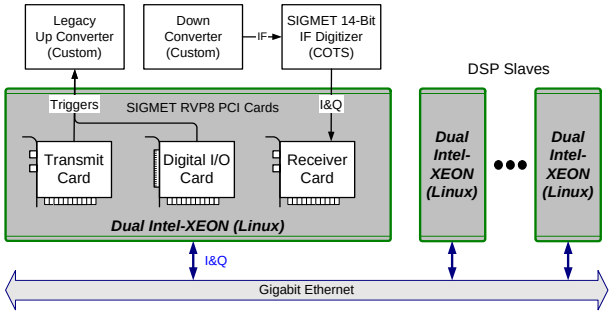

Figure 2. The new RDA uses a cluster of Linux PCs for digital signal processing.

Although a single dual-processor system is sufficient to implement the legacy signal processing algorithms (requiring less than 250 MFLOPS), future algorithms will require additional processors. The enhanced architecture uses a cluster of COTS compute servers connected via gigabit Ethernet to provide broad scalability to meet the future computational requirements. The in-phase and quadrature (I&Q) data is distributed to a selectable number of DSP slaves using a software standard called Message Passing Interface (MPI). Since all of the software is designed for standards-based interfaces, the final choice of hardware brand and model can be made just before deployment to take advantage of increases in processor speed.

The engineering prototype of the RDA was installed in July 2003 at FAA's Oklahoma City Program Support Facility (PSF) site. FAA personnel are currently evaluating and testing an initial configuration that provides hardware replacement of the RDA platform and implements the existing DSP algorithms in software. In 2005, this initial configuration will be fielded at one or two operational TDWR sites. This will provide an opportunity to record I&Q data to facilitate the algorithm development effort. Algorithmic improvements such as those discussed below will then be inserted into the platform in 2005-2006, potentially in parallel with operational deployment of the new RDA design.

3. ADAPTIVE RV MITIGATION SCHEME

In the current TDWR operational system, an adaptive approach is already used. At the lowest tilt, information from an initial long-PRI scan is used to determine the optimal PRIs of the next two scans (conducted at the same elevation). The two PRIs are selected to minimize range overlay in a specified region around the airport and provide velocity dealiasing via the Chinese remainder theorem. However, because the PRI is constant for each scan, the range overlay protection capability is very limited. A PRI that protects well for a given azimuth and range does not necessary provide any protection at other azimuths and ranges.

We propose a more powerful technique that enhances range overlay protection for all azimuths and range gates. Selection between two different waveform and processing schemes will be made on a radial-by-radial basis based on the initial long-PRI scan. The two techniques, multi-PRI (Cho et al., 2003) and phase-code processing (e.g. Siggia, 1983), have complementary characteristics for range-fold protection depending on the overlay type (Fig. 3).

Out-of-trip Signal Type / Technique	High Power or Wide Spectrum	Long Contiguous Range Extent
Multi-PRI Processing	Yes	No
Phase Code Processing	No	Yes

Figure 3. Overlay protection capability

A simplified summary of the selection algorithm is shown in Fig. 4. For a given radial, the algorithm looks at each range gate i and assigns a score of –1 or 1 to multi-PRI ($S_{MP}(i)$) and phase code ($S_{PC}(i)$), depending on whether the respective approaches will protect this gate from overlays. Then the scores are summed over all gates with weighting factor $W(i)$, which depends on the gate's location relative to the airport and approach and departure corridors (the highest priority areas). The waveform and processing type is chosen based on the aggregate scores. For the example that we present below, $W(i)$ is just set proportional to range, since the area of the range-azimuth display "pixels" is proportional to range. Note that there is an additional complication not shown in Fig. 4, which is that sometimes two consecutive radials need to be examined simultaneously because velocity dealiasing for phase code processing requires that the PRI be switched between two values every other radial.

4. VELOCITY DEALIASING

For a multi-PRI waveform, there are different approaches to velocity dealiasing. The approach that we choose is first constrained by the range of PRIs available. This range is bounded by signal coherency (for accurate velocity estimation) on the upper end (~1000 μs) and by the FAA's range coverage requirement of 48 nautical miles on the lower end (594 μs). Then, for maximum range-overlay protection for various scenarios, the PRIs should be spread out more-or-less evenly throughout this range. Another constraint is that the "raw" velocity estimates must be made for each PRI set separately and not coherently over all PRI sets, because one or more of the PRI sets may be contaminated by range-folded echoes and

need to be thrown out. Clearly, the variance of the velocity estimate will be larger compared to that of an equivalent dwell of constant-PRI pulses, but this is the price to pay for the aggressive range-fold protection and velocity dealiasing capability provided by multi-PRI processing. This is why the phase code processing is the default choice if there is no range folding in a given radial.

Taking these considerations into account we selected the following sequence of PRIs for initial implementation of the multi-PRI waveform: 597, 630, 672, 709, 796, 840, 896, 945 μs, with each PRI having eight consecutive pulses totaling 64 pulses. We call this type of configuration a multi-block-staggered (MBS) PRI sequence. The number of consecutive pulses can be adjusted based on the antenna rotation rate. In this PRI set there are seven pairs of simple integral ratios (2 x 2:3, 4 x 3:4, and 1 x 4:5) that can be employed for velocity dealiasing. The minimum unfolded velocity interval provided by these pairs is 42 m s^{-1}, which satisfies the FAA's required velocity range of 40 m s^{-1}.

The velocity estimation procedure is as follows. First, pulses that are too contaminated by overlaid signals are eliminated. Velocities are computed for the remaining PRI subsets. If there is at least one of the simple integral ratio pairs still available, unfolded velocities are computed for each pair, and the median taken over all the results. If there are no remaining simple integral ratio pairs, but there is still more than one PRI subset left, then an unfolded-velocity-matching algorithm (Trunk and Brockett, 1993) is used to compute the dealiased velocity. If only one clean PRI subset remains, then velocity dealiasing is not attempted.

As mentioned earlier, since constant-PRI phase-code processing does not provide velocity dealiasing, the PRI is switched between two values in a simple integral ratio on consecutive radials. Unfolded velocities are computed based on the interradial velocity difference if both values are clean from range folding.

5. GROUND CLUTTER FILTERING

For a constant-PRI waveform, ground clutter can be filtered in the spectral domain in some adaptive fashion. Our current filter is based on SIGMET's Gaussian model adaptive processing (GMAP) filter (Siggia and Passarelli, 2004). Clutter filtering a multi-PRI signal is more problematic, because power from nonzero Doppler frequencies are aliased to the ground clutter band around zero. Thus, clutter filtering also removes power from the aliased frequencies and distorts the phase response at those frequencies. The phase distortion in turn leads to degradation of velocity estimates.

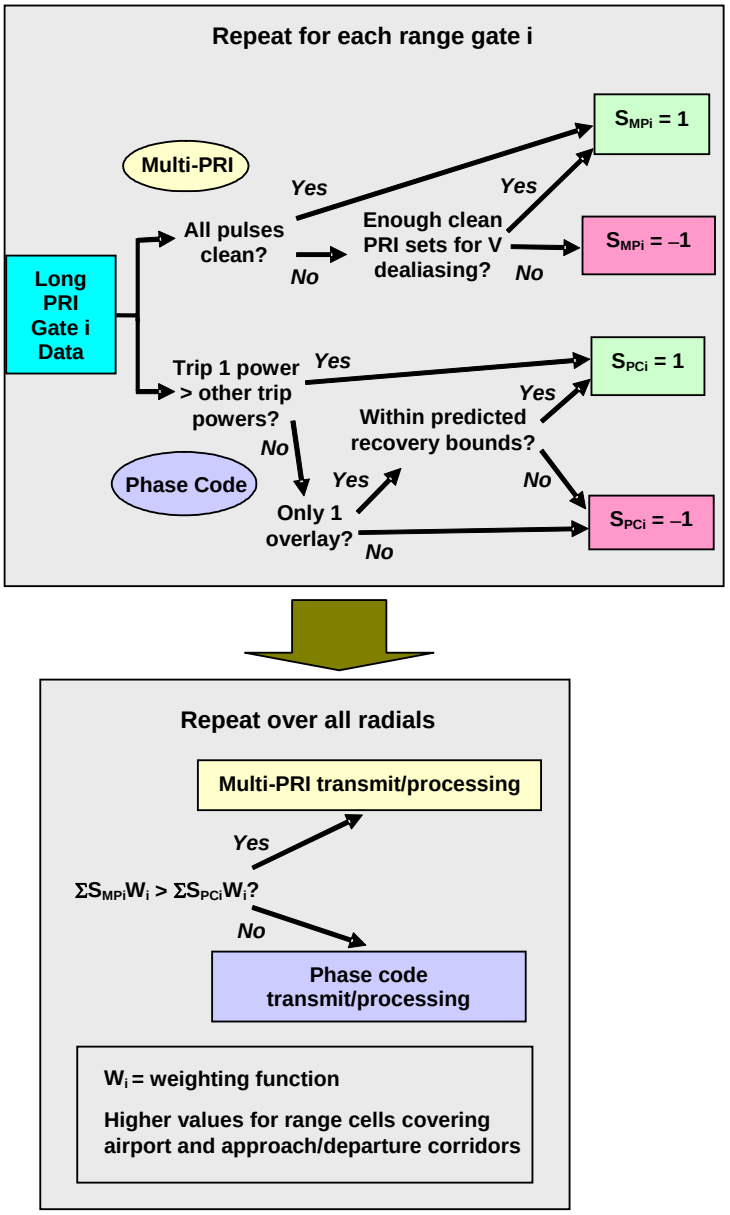

Figure 4. Diagram of adaptive waveform and processing selection algorithm.

To solve this problem, a finite impulse response (FIR) clutter filter design yielding an excellent balance of magnitude response and phase linearity was introduced by Chornoboy (1993) for block-staggered PRI waveforms. Filters using this design algorithm are employed in the operational Weather Systems Processor (WSP) channel of the ASR-9 (Weber, 2002) for dual-PRI signals. The same design algorithm can be used for MBS signals. Fig. 5 shows the characteristics of a clutter filter designed for the MBS sequence defined in the previous section. The stop-band full width is 1.8 m s^{-1} and the clutter suppression is 60 dB for an antenna rotation rate of 19° s^{-1}.

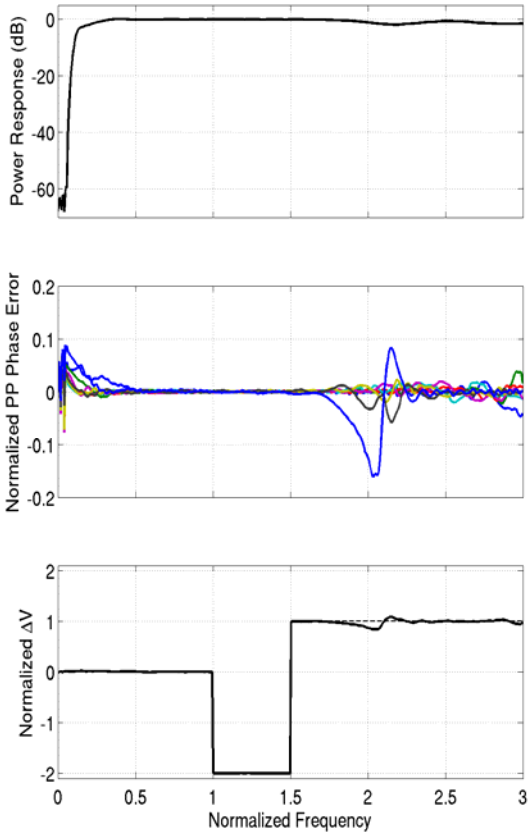

Figure 5. Power response of the multi-PRI clutter filter (top). Frequency is normalized by the Nyquist frequency of the longest PRI. Pulse-pair phase error vs. normalized frequency for each PRI subset (middle). Phase errors are normalized by π. Difference between velocity computed from PRI = 945 and 630 μs (bottom) for no phase errors (dashed) and with phase errors (solid). The difference is normalized by the Nyquist velocity corresponding to the longest PRI.

The frequency range in Fig. 5 corresponds to 42 m s^{-1} in velocity. The magnitude response is quite flat in the pass band. The pulse-pair phase error also does not exceed ~5% of π in the pass band, except for one PRI subset. For velocity unfolding with the Chinese remainder theorem, it is important that the phase distortion not cause the velocity difference between PRI pairs to be identified with the incorrect quantized value; otherwise, false unfolding results. The velocity differences for the worst-case simple integral ratio PRI pair are shown in the bottom of Fig. 5. We see that the phase errors will not result in false unfolding.

Note that clutter filtering interferes with the protection of a weak signal in the same trip against a stronger signal overlaid from another trip. This is true for both phase-code and multi-PRI processing. Therefore, clutter filtering should only be applied when necessary. For phase-code processing, the amount of clutter present can be deduced from the adaptive clutter filter output. For multi-PRI, the presence of ground clutter can be checked by the use of a clutter residue map or from the combination of long-PRI clutter data (obtained from an adaptive spectral-domain filter) and an iterative multi-filter scheme. The latter approach, which is used here, will also protect against anomalous propagation.

6. EXAMPLE RESULTS

To illustrate the performance of our adaptive RV ambiguity mitigation scheme, we show the results of processing simulated weather I&Q data in Fig. 6.

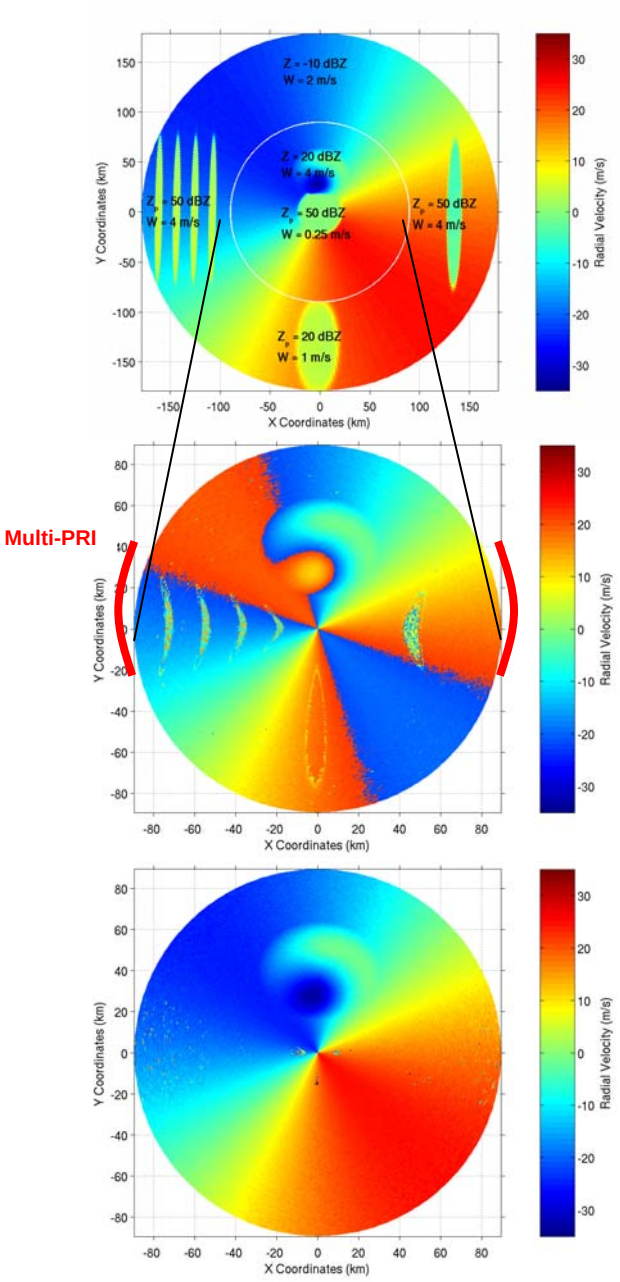

Figure 6. PPI velocity plot of the simulated input with reflectivities and spectral widths of the background, clutter, and weather patches shown in text (top). Velocity for single-PRI (597 ms), no phase-code processing (middle). Velocity for adaptive RV mitigation algorithm (bottom).

The simulation consisted of a constant-reflectivity background plus five "patches" meant to mimic ground clutter (center) and microburst (north) in the 1st trip, and weak, range-extensive overlay (south), strong, range-sparse overlays (east and west) from the 2nd trip. The clutter and overlay patches had 2D Gaussian reflectivity distributions. The middle plot shows the result for a single-PRI waveform with no phase-code processing. The bottom plot shows the result using our adaptive RV mitigation algorithm. The first-trip protection and velocity dealiasing worked very well except where there was both ground clutter and range folding. Not shown here due to limited space are the separate results for multi-PRI and phase-code processing that show the former failing on the southern overlay and the latter not filtering out the eastern and western overlays. In this case, the selection algorithm made exactly the right choices as indicated by the red lines.

7. SUMMARY

The TDWR receiver and signal processor are being upgraded to provide a platform for new algorithms that will improve the quality of the base data. We formulated an adaptive selection algorithm for choosing between multi-PRI and phase-code processing on a radial-by-radial basis by using information from an initial long-PRI scan. Results on simulated data show promise in mitigating RV ambiguity. Results of processing real data off-line also show good promise. The upgraded RDA will eventually allow real-time adaptive processing. Other types of waveforms and processing techniques could easily be added in the future, thus ensuring flexibility in devising further data quality improvement schemes.

8. REFERENCES

Cho, J. Y. N., G. R. Elkin, and N. G. Parker, 2003: Range-velocity ambiguity mitigation schemes for the enhanced Terminal Doppler Weather Radar. Preprints, *31st Conf. on Radar Meteorology*, Amer. Meteor. Soc., 463-466.

Chornoboy, E. S., 1993: Clutter filter design for multiple-PRT signals. Preprints, *26th Conf. on Radar Meteorology*, Amer. Meteor. Soc., 235-237.

Siggia, A., 1983: Processing phase coded radar signals with adaptive digital filters. *Preprints, 21st Conf. on Radar Meteorology*, Amer. Meteor. Soc., 167-172.

Siggia, A. D., and R. E. Pasarelli, Jr., 2004: Gaussian model adaptive processing (GMAP) for improved ground clutter cancelation and moment estimation. Preprints, *3rd European Conf. on Radar in Meteorology and Hydrology*, Visby, Sweden, Copernicus Gesellschaft.

Trunk, G., and S. Brockett, 1993: Range and velocity ambiguity reduction. Preprints, *1993 IEEE National Radar Conf.*, 146-149.

Weber, M. E., 2002: ASR-9 Weather Systems Processor (WSP) signal processing algorithms. *LL ATC-255*, MIT Lincoln Laboratory, Lexington, MA, 53 pp.